water

MDPI

Article

Sediment Transport Processes in the Kelani River Basin, Sri Lanka: Formation Process of Bed Material Size Distribution

Pavithra Sudeshika Dissanayaka Mudiyanselage [1,*], Daisuke Harada [2], Yoshiyuki Imamura [1,*] and Shinji Egashira [2]

[1] Department of Civil and Environmental Engineering, Tokyo Metropolitan University, Hachioji 192-0397, Japan
[2] International Centre for Water Hazard and Risk Management (ICHARM), Public Water Research Institute (PWRI), Tsukuba 305-8516, Japan; harada@icharm.org (D.H.); egashirasn@mail2.accsnet.ne.jp (S.E.)
* Correspondence: pavithrasudeshi@gmail.com (P.S.D.M.); imamura@tmu.ac.jp (Y.I.)

Abstract: This study investigates sediment transport processes in the Kelani River Basin, Sri Lanka, focusing on the formation of bed material sediment size distributions. Sediment transport processes during the flood events in 2016 and 2018 are evaluated using two approaches: assuming an equilibrium condition (Case 0) and evaluating basin-scale sediment transport using a distributed Rainfall–Sediment–Runoff (RSR) model based on the unit channel (Cases 1 and 2). Case 1 considers sediment transport only inside river channels, while Case 2 considers sediment supply at upstream end unit channels. The results indicate significant sediment deposition in the downstream reach, particularly downstream of Location 7. In Case 1, the sediment size distribution downstream rapidly coarsens, while in Case 2, considering sediment supply, the bed sediment size distribution downstream is close to the observed one, regardless of flood magnitude. This suggests that with sufficient sediment supply, the bed sediment size distribution forms based on channel conditions such as width and slope. Case 0 shows a similar trend in sediment transport rate to Case 2, demonstrating the applicability of this simple approach. In conclusion, this study has revealed the formation process of the present sediment bed conditions, which provides insight into effective and sustainable river management, including sand mining activities.

Keywords: Kelani River Basin; rainfall–sediment–runoff; sediment transport processes; sediment sorting; sediment grain size distribution

check for updates

Academic Editor: Karol Plesiński

Received: 20 March 2025
Revised: 14 May 2025
Accepted: 26 May 2025
Published: 2 June 2025

Citation: Dissanayaka Mudiyanselage, P.S.; Harada, D.; Imamura, Y.; Egashira, S. Sediment Transport Processes in the Kelani River Basin, Sri Lanka: Formation Process of Bed Material Size Distribution. *Water* **2025**, *17*, 1683. https://doi.org/10.3390/w17111683

Copyright: © 2025 by the authors. Licensee MDPI, Basel, Switzerland. This article is an open access article distributed under the terms and conditions of the Creative Commons Attribution (CC BY) license (https://creativecommons.org/licenses/by/4.0/).

1. Introduction

The Kelani River is Sri Lanka's second-largest water resource, supporting 20% of the nation's population [1] and significantly contributing to the country's economic prosperity as it flows through the capital of the country. This vital waterway supplies 80% of Colombo's drinking water requirements [2], generates hydroelectric power in its upper reaches, and sustains crucial aquatic ecosystems [3] and biodiversity within the basin [4]. However, extensive sand mining has resulted in the erosion of the riverbed and banks, causing an annual decline of approximately 10 cm in riverbed elevation [5]. In the downstream reach of the Kelani River, approximately 6 m of riverbed degradation has been observed since 1961 [6]. Consequently, saltwater intrusion now extends to the Ambatale water treatment facility, degrading water quality and posing a threat to the river's aquatic life [3]. Therefore, it is imperative to implement sediment management strategies in the Kelani River to re-establish the river's sustainability.

The distribution of sediment grain sizes in riverbeds plays a crucial role in understanding fluvial hydraulics, sediment transport dynamics, and river morphology [7,8]. This

distribution undergoes continuous alteration in natural watercourses, both temporally and spatially, due to ongoing sediment exchange, deposition, and erosion within river channels [9]. Modifications in bed material can influence bed roughness, subsequently affecting flow patterns. Moreover, the sediment grain size distribution impacts the sediment transport capacity, leading to longitudinal and transverse sorting patterns [10]. These variations in sediment transport directly influence the deposition and erosion trends observed in river channels [11,12]. Furthermore, the distribution of sediment particle sizes plays a role in forming stable river cross-sections [13] and affects the habitat conditions for communities of macroinvertebrates [14,15]. Therefore, understanding the grain size distribution of bed material forms is essential for various management practices such as the sustainable development, maintenance, and restoration of rivers and estuaries.

The geometry of river channels and the size of sediment grains are fundamentally connected to the amount of sediment transported from upstream areas [16]. The supply of sediment is influenced by various events, including landslides, debris flows, swift bank erosion, or sediment movements involving hillsides, riverbanks, tributaries, riverbeds, or upstream areas [7]. Flume tests by Venditti et al. [17] demonstrate that pulses of coarse sediment result in a finer bed surface and coarser bed load. Conversely, pulses of finer sediment also lead to a finer bed surface, but in gravel-bed rivers, they cause the bed load to become finer as well. A study conducted by Buffington and Montgomery [18] utilising a flume apparatus indicates that an inverse relationship exists between the median grain size of the bed surface and the rate at which sediment is supplied in an equilibrium gravel channel. The behaviour of sediment pulses in gravel-bedded channels has garnered considerable attention, resulting in numerous flume experiments [17,19] and one-dimensional numerical simulations [20]. This research explores how rivers form their bed material size distribution in response to the absence or presence of sediment input from the uppermost tributaries. The study focuses on uppermost tributaries that maintain equilibrium sediment transport throughout flood events, examining their influence on downstream sediment transport processes using numerical simulations.

To investigate the formation processes of riverbed material size distribution, this study employs a distributed Rainfall–Sediment–Runoff (RSR) model. The RSR model conceptualises the river network as a series of interconnected unit channels, introduced by Egashira and Matsuki [21], each representing a channel between confluences. By evaluating sediment inflow and outflow in terms of bedload and suspended load for each unit channel and connecting them across the entire basin, the RSR model calculates basin-scale sediment runoff [22,23]. The bed shear stress at each unit channel is evaluated based on flood discharges obtained from a distributed rainfall–runoff calculation. The RSR model simulation allows a relatively precise evaluation of the dynamic changes in riverbed elevation and bed material grain-size distribution during the flood event.

This study aims to investigate sediment transport processes in the Kelani River Basin, specifically focusing on the formation processes of bed material sediment size distribution to contribute to improved sediment management in the Kelani River. Sediment transport processes during the 2016 and 2018 floods are calculated to understand how sediment supply, sediment transport, and local flow conditions interact to form the present bed environment, characterised by the present sediment size distributions. This study evaluates sediment transport during the flood events that occurred in May 2016 and May 2018 by comparing the results of three calculation approaches: one assuming an equilibrium condition (Case 0), and the other two by evaluating basin-scale sediment transport using a distributed Rainfall–Sediment–Runoff (RSR) model based on the unit channel (Cases 1 and 2). Case 1 considers sediment transport only inside the river channels, while Case 2 considers sediment supply at the upstream end unit channels.

2. Study Area and Data Set

This study focuses on the Kelani River Basin, depicted in Figure 1A, which is situated between latitudes 6°47′ and 7°05′ and longitudes 79°52′ and 80°13′, extending from the central hill region to Colombo, encompassing an area of 2230 km^2 [24]. One-third of the Kelani River Basin area is occupied by rubber cultivation, 24.6% comprises homesteads, 10.2% is forested, and 11.8% is covered by tea cultivation [25]. The catchment receives a substantial amount of rainfall, as it is entirely located within the wet zone of the country. The average annual rainfall is approximately 3718 mm. While the Southwest monsoon provides a major portion of the yearly rainfall, the northeast monsoon and periods between monsoons also make substantial contributions to total precipitation [26]. During the monsoon period, the water flow varies between 600 and 1800 m^3 [24]. The upstream region is characterised by steep terrain, whereas the downstream area below Hanwella is predominantly flat [27]. The lower basin exhibits a high vulnerability to flooding. The most recent severe flood occurred in 2016. This study considers two flood events, including the 2016 flood event and a moderate flood event that occurred in 2018. Figure 1B illustrates the riverbed elevation profile measured by the Irrigation Department in 2016 and the channel width based on measured cross-sections in 2016 and Google satellite images, with locations denoted as 1 to 11 in Figure 1A. As shown in Figure 1B, the downstream bed slope from Locations 1 to 7 is approximately 0.000055, whereas the upstream bed slope from Location 7 and above is approximately 0.0005. The average downstream channel width is approximately 80 m, whereas the average upstream channel width is approximately 60 m. Figure 1C shows the sediment grain size distribution of the riverbed material at Locations 1 to 11. The "merged downstream" shows the average of the field-measured average sediment grain size distribution from Locations 1 to 7, whereas "merged upstream" shows the field-measured average sediment grain size distribution from Locations 8 to 11. The sediment samples were collected in January/February 2023 from the middle of the river and in proximity to the riverbank at each cross-section using a scraper bucket sampler with a long handle. According to Figure 1C, the mean diameter of the downstream region is approximately 0.45 mm, while the upstream mean diameter is approximately 1 mm.

Additional data utilised for this investigation comprise 15-arc (500 m) HydroSHEDS (Hydrological data and maps based on Shuttle Elevation Derivatives at multiple scales), hourly discharge data at Glencourse and Kithulgala obtained from the Irrigation Department, hourly rainfall data from seven locations (Colombo, Hanwella, Glencourse, Deraniyagala, Kithulgala, Holombuwa, and Norwood) provided by the Irrigation Department and Meteorological Department, and hourly turbidity data supplied by the National Water Supply and Drainage Board.

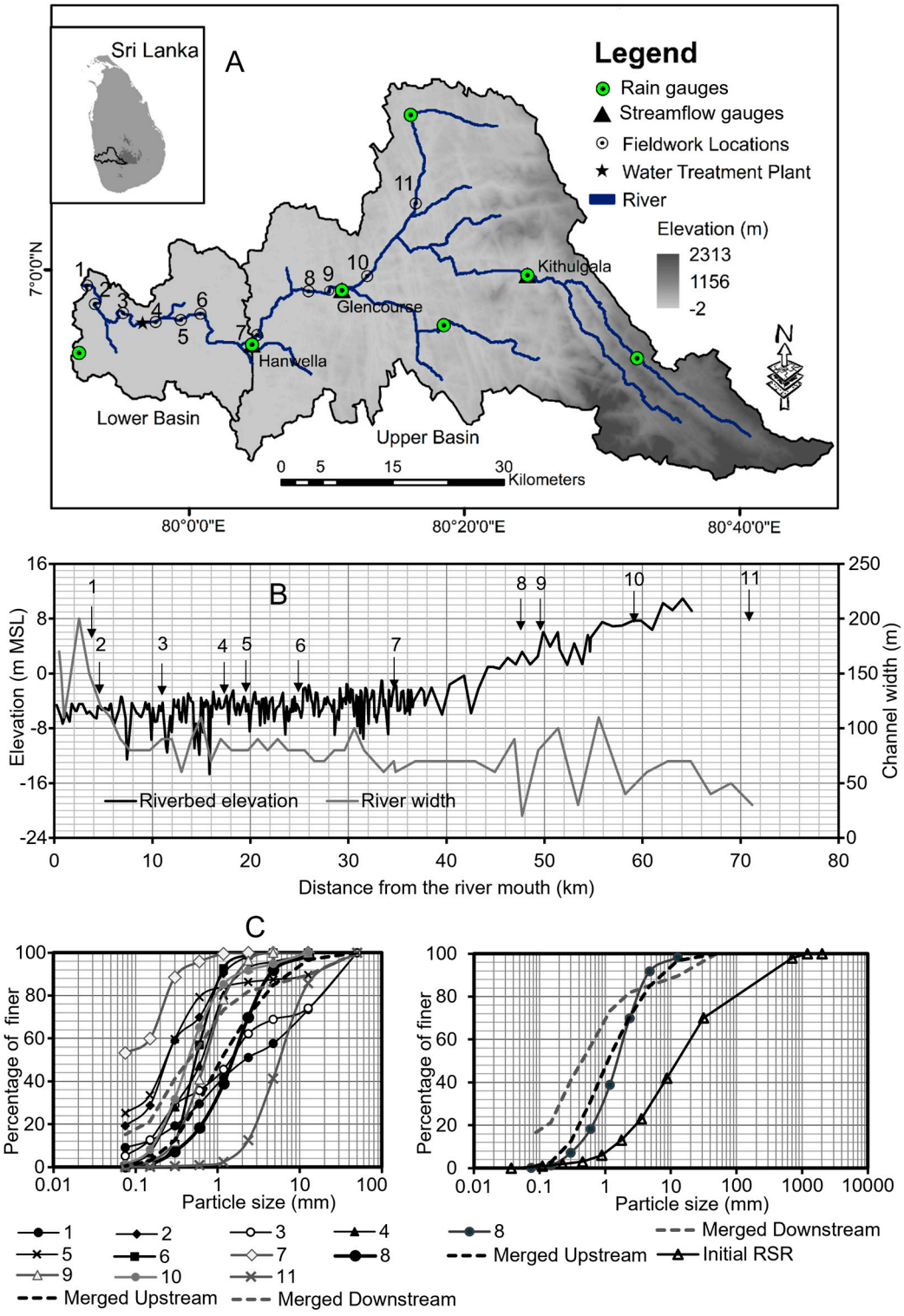


Figure 1. (**A**) Study map of the Kelani River Basin. (**B**) Longitudinal profiles of riverbed elevation and channel width with fieldwork Locations 1–11. (**C**) Sediment size distribution curves at fieldwork Locations 1 to 11.

3. Methodology

This study employs the Rainfall–Sediment–Runoff (RSR) model to understand the characteristics of sediment transport in the Kelani River Basin. In this method, the river network is conceptualised as a series of unit channels. A unit channel is a river segment located between two tributaries with two inflow entry points and one outflow point, as

shown in Figure 2. In addition, this study evaluates sediment transport rates assuming an equilibrium condition. This section introduces these methodologies.

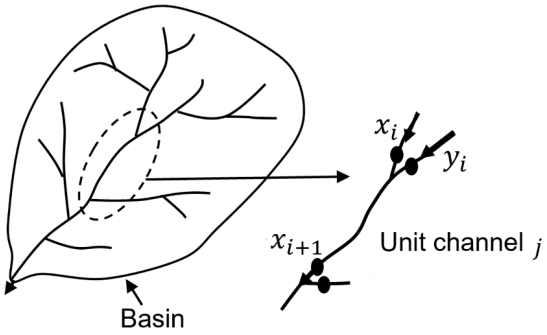


Figure 2. Definition of a unit channel.

3.1. Formulas to Evaluate the Bedload Rate and Suspended Sediment Concentration

The evaluations of the bedload transport rate and suspended sediment concentration are keys when evaluating bedload and suspended load with rainfall runoff at a given cross-section of the channel network in a drainage basin. First, regarding the bedload formulas, there are three types, such as the 3/2-power of non-dimensional bed shear stress like Mayer–Peter and Muller's formula [28], the 5/2 power of non-dimensional bed shear stress like Brown's formula [29], and the intermediate between the two. The bed load rate computed by the 3/2 power type formula does not depend on sediment particle sizes, and the 5/2 power type formula gives the transport rate that increases proportionally with the decrease in sediment particle size. We adopt the 5/2 power type, which makes it easy to evaluate the sediment sorting processes and apply Egashira et al.'s equation [30,31], which is derived by applying the constitutive relations of the water–sediment mixture to the bedload layer.

$$q_{b*} = 4/15K_1^2K_2/\sqrt{f_f + f_d}\tau_*^{5/2} \quad (1)$$

where $K_1 = 1/cos\theta 1/tan\phi - tan\theta$, $K_2 = 1/c_s$, $f_f = 0.16$, and $f_d = 0.0828(1-e^2)(\sigma/\rho)c^{1/3}$. q_{b*} is the non-dimensional bedload rate defined as $q_{b*q_b/\sqrt{(\sigma/\rho-1)gd^3}}$, τ is the non-dimensional bed-shear stress defined as $\tau = hi/(\sigma/\rho-1)d$, ($i$ is the energy slope), θ is the bed slope, ϕ is the internal friction angle of sediment particles, h_s is the thickness of the bedload layer, h is the flow depth, c_s is the sediment concentration of the bedload layer and approximated by $c_s = c/2$ (c is the sediment concentration of the stationary layer), e is the restitution, σ is the mass density of sediment particles, and ρ is the mass density of water. For simplicity, using the values and conditions such as $cos\theta = 1$, $tan\theta \ll 1$, $c_s = c/2 = 0.26$, $\sigma/\rho = 2.65$, $e = 0.85$, $\varnothing = 34°$, and $K_2 = 1/c_s = 3.85$ ($\left(1-h_s/h\right)^{1/2} \doteq 1$), Equation (1) can be simplified as

$$q_{b*} = 4.4\tau_*^{5/2} \quad (2)$$

This simplified formula is applied to the bedload computations later.

On the other hand, for suspended sediments, if the erosion rate of the bed material in unit time and unit area and the deposition rate of suspended sediment on the riverbed can be reasonably formulated, the following convection equation can be used to evaluate the suspended sediment concentration.

$$\partial ch/\partial t + 1/B\partial cvB/\partial x = E - D \quad (3)$$

where c is the cross-sectional average concentration of suspended sediment, h is the flow depth, v is the cross-sectional average velocity, B is the flow width, E is the entrained

sediment volume in unit time and unit area, and D is the deposition sediment volume in unit time and unit area.

In evaluating E, most research has employed the idea that the settling sediment volume should be balanced with the upward transporting sediment volume due to turbulent diffusion. This study employs the method developed by Harada et al. [32], taking into account the non-equilibrium characteristics of the suspended sediment, in which the entrainment rate is formulated by considering that the suspended sediment originates from the entrainment of the bedload layer. This is expressed as follows.

$$E = W_e c_s \tag{4}$$

where W_e is the entrainment velocity which they evaluated using the result obtained from the flume tests on density-stratified flows [33].

$$W_e/v = K/R_{i*}, \ \left(R_{i*(\sigma/\rho-1)c_s gh/v^2}\right) \tag{5}$$

where R_{i*} is the Richardson Number, K = 0.0015. In addition, the deposition rate of the suspended sediment is assumed to be applicable.

$$D = w_0 c \tag{6}$$

where w_0 is the fall velocity of the suspended sediment. Harada et al. obtained an expression of the equilibrium concentration of the suspended sediment using the relation of $E = D$ and Equation (4):

$$c_e = K/(\sigma/\rho - 1)v/w_0 F_r^2, \ \left(F_r = v/\sqrt{gh}\right) \tag{7}$$

where F_r is the Froude Number.

In the computations by rainfall runoff and sediment runoff (RSR model), Equation (2) for the bedload and Equation (3) together with Equations (4) and (6) for the suspended load are employed. In addition, we compute the suspended load using Equation (7) assuming that an equilibrium transportation is accomplished in comparison to the results obtained from the RSR model. The formulas illustrated in Equations (2) and (3) and associated formulas, and Equation (6) are modified when we apply them to non-uniform sediment.

3.2. Sediment Transport Rates with RSR Model

The RSR model evaluates rainfall–runoff processes for each cell in a Cartesian grid system, whereas sediment transport processes are evaluated using the unit channel model, as illustrated in Figure 2.

The unit channel features two entry points at the upstream junction (x_i, y_i) and a single exit point at the downstream junction (x_{i+1}). The continuity equation for the water flow is as follows,

$$\partial h_j/\partial t = 1/B_j L_j\left[Q(x_i) + Q(y_i) - Q(x_{i+1}) + q_{i+1}L_j\right] \tag{8}$$

where, h_j, B_j, and L_j represent the flow depth, width, and length of the unit channel j, respectively, t denotes time, q_{i+1} is the lateral inflow discharge per unit length into the unit channel, and Q is flow discharge which is determined using a kinematic wave approximation which is expressed as $Q =$, where n is Manning's roughness coefficient, i is the bed slope, h is the flow depth, and B is the flow width.

The convection equation for the transport of suspended sediment in the unit channel j is,

$$\begin{aligned}\partial hc_i(x_{i+1})/\partial t = (1/B_jL_j)\{c_{si}(x_i)Q(x_i) + c_{si}(y_i)Q(y_i) - c_{si}(x_{i+1})Q(x_{i+1})\} \\ -D_{si}(x_{i+1}) + E_{si}(x_{i+1})\end{aligned} \quad (9)$$

where c_i is the suspended sediment concentration for the sediment size class i, c_{si} is the sediment concentration for the sediment size class i, D_{si} is the deposition rate of the suspended sediment for the sediment size class i which is given by $D_{si} = w_{oi}c_i$, where w_{oi} is the settling velocity of the sediment, E_{si} is the erosion rate of the suspended sediment for the sediment size class i, which is given by $E_{si} = W_e f_{bi} c_s$ [34], where f_{bi} is the fraction of the sediment size class i, c_s is the sediment concentration of the bedload layer, and W_e is the entrainment velocity, which is given by $W_e/v = K/R_{i*}$ [33], where R_{i*} is the overall Richardson number given by $R_{i*(\sigma/\rho-1)c_s gh/v^2}$, v is the spatial average velocity, and K is consistent with its definition in Section 3.1.

The mass conservation equation for the bed sediment in the unit channel j is as follows,

$$\partial Z_b/\partial t = (1/(1-\lambda))\sum_i [(1/B_jL_j)\{Q_{bi}(x_i) + Q_{bi}(y_i) - Q_{bi}(x_{i+1})\} + D_{si}(x_{i+1}) - E_{si}(x_{i+1})] \quad (10)$$

where Z_b is the riverbed elevation, λ is the porosity of the bed sediment, Q_{bi} is the bedload rate for the sediment size class i, which is determined by Egashira et al.'s formula given by $q_{b*i} = 4.4 p_i \tau_i^{5/2}$, where q_{b*i} is the non-dimensional bedload rate in unit time and unit length for the sediment size class i, and τ_i is the non-dimensional bed shear stress for the sediment size class i. The bedload rate per unit time and unit length for the sediment size class i is denoted by q_{bi}, which is calculated by $q_{bi} = q_{b*i}\sqrt{(\sigma/\rho - 1)g d_i^3}$.

The temporal changing rate of sediment grain size fraction for the surface layer for the sediment class i is as follows,

$$\begin{aligned}\partial P_i/\partial t = (1/(1-\lambda)\delta B_jL_j)\{Q_{bi}(x_i) + Q_{bi}(y_i) - Q_{bi}(x_{i+1})\} + D_{si}(x_{i+1}) \\ -E_{si}(x_{i+1}) - (\partial z/\partial t)(f_i/\delta)\end{aligned} \quad (11)$$

where $\sum_1^N p_i = 1$, $f_i = \begin{cases} p_{i2}\ when\ \partial z/\partial t \le 0 \\ p_i when \partial z/\partial t > 0 \end{cases}$

p_i is the fraction of the sediment size class i, δ is the depth of the surface layer, which is the exchange layer or bedload layer, and p_{i2} is the fraction of the sediment size class i in the second layer underneath the exchange layer.

The RSR model is prepared for the Kelani River Basin utilising the 15-arc HydroSHEDS Digital Elevation map, with rain gauge data from seven locations as presented in Figure 1A, establishing the initial sediment distribution as illustrated in Figure 1C, and incorporating upstream boundary discharge at Kithulgala using the observed streamflow data. River geometry is defined in relation to the upstream contributing area: $Channelwidth = 1.8A^{0.5}$ and $Channeldepth = 5A^{0.05}$, where A represents the upstream contributing area in km^2. In the present study, the sediment supply at the uppermost unit channels is not considered. The variables utilised in the RSR model include a mesh size of 500 m, a specific gravity of sediment (σ/ρ) of 2.65, and 12 sediment size classes. The calibrated Manning's roughness coefficient of the river, and the equivalent roughness of slope, soil depth, soil porosity, and saturated hydraulic conductivity are 0.04, 0.85, 1 m, 0.4, and 0.09 m/s, respectively.

The model calibration and validation were carried out for the flood events that occurred in May 2016, May 2017, and May 2018 using the hourly sediment data at the Ambatale Water treatment Plant, which is the only location where hourly sediment is monitored in the Kelani River. Additionally, hourly streamflow data at Location 9, which is

located in the middle region of the watershed, was utilized due to its data availability, ease of validation, and data quality such as no backwater or tidal effects. Figure 3 shows the calibration and validation results for the RSR model. Figure 3A compares the simulated flood hydrograph calculated using the RSR model with the observed discharge at Location 9 for the 2016, 2017, and 2018 flood events. Figure 3B depicts the simulated suspended sediment concentration compared with the measured suspended sediment concentration at the Ambatale water treatment plant during the aforementioned flood events. The observed hourly sediment concentration data at the Ambatale water treatment plant is based on hourly turbidity measurements taken using the portable turbidity meter HACH 2100 P by the National Water Supply and Drainage Board. The relationship between turbidity (in NTU) and the total suspended solids concentration (in mg/L) is described by the linear regression equation $y = 3x + 3$, with a Pearson correlation coefficient of 0.63, based on the observed turbidity and total suspended sediment concentration measurements during 2016–2020 by the National Water Supply and Drainage Board. As shown in Figure 3A,B, the RSR model demonstrates an accurate prediction in terms of flow discharge and suspended sediment concentration. Figure 3B shows that the calculation results underestimate the peak sediment concentration for the 2016, 2017, and 2018 floods. This is likely attributable to the removal of temporary sandbags barrier at the Ambatale water treatment plant, which are typically used to prevent saltwater intrusion during the dry season. The Mean Error (ME), Root Mean Square Error (RMSE), and Pearson correlation coefficient (R^2) for the simulated flood hydrographs and sediment concentrations for the 2016, 2017, and 2018 floods are presented in Table 1. The results confirm that the model's performance is satisfactory.

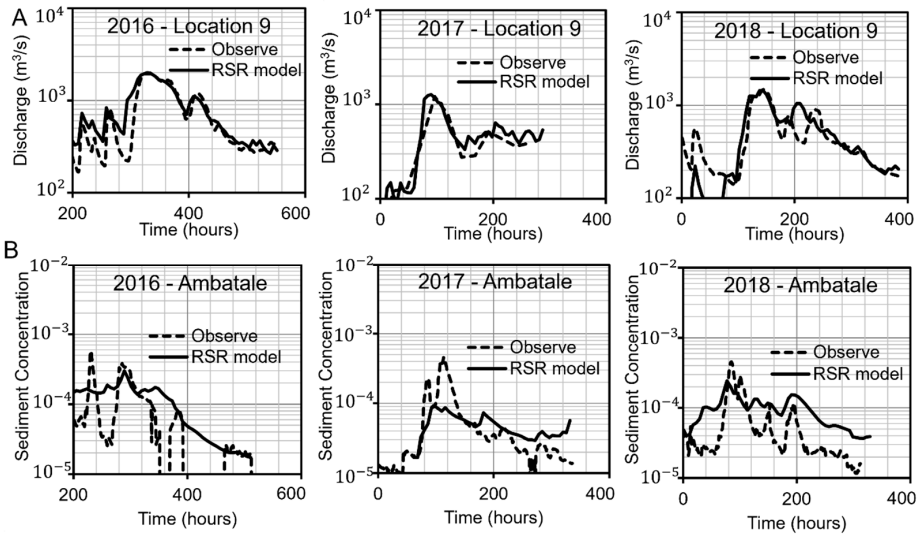


Figure 3. (**A**) Simulated flood hydrograph, (**B**) Simulated sediment concentration by the RSR model with observed data for the 2016, 2017, and 2018 flood events.

Table 1. Mean Error (ME), Root Mean Square Error (RMSE), and Pearson correlation coefficient (R^2) for the simulation results by the RSR model.

Performance Indices	ME	RMSE	R^2
• Flood hydrograph			
Flood in 2016	−95	192	0.95
Flood in 2017	−58	122	0.94
Flood in 2018	−76	212	0.85
• Sediment concentration			
Flood in 2016	-3.2×10^{-5}	8.5×10^{5}	0.66
Flood in 2017	2.0×10^{-5}	8.2×10^{-5}	0.68
Flood in 2018	-3.6×10^{-5}	6.9×10^{-5}	0.67

4. Comparison of Sediment Transport Estimations with No Bed Variations and the RSR Model

4.1. Sediment Transport Rates

This section compares the sediment transport estimations with no bed variations and the numerical simulation results obtained by the RSR model. In this context, Case 0 refers to sediment transport estimations with no bed variations, while Case 1 represents sediment transport estimations by the RSR model. The Case 0 sediment transport estimation with no bed variation utilises observed discharge hydrographs at Locations 7 and 9 and the observed average upstream and downstream sediment grain size distributions in Figure 1C for the estimations. The bed slope at Location 7 (downstream) is set to 0.000055 with a flow width of 80 m. At Location 9 (upstream), the bed slope is set to 0.0005, and the flow width is 60 m. In Case 1, the RSR model considers sediment transport throughout the entire basin, whereas Case 0 sediment transport estimations with no bed variations assume that the sediment size distribution remains constant over time. The difference between Case 0 and Case 1 represents the non-equilibrium of the sediment transport processes.

Figure 4 compares the bedload and suspended load rates for Cases 0 and 1 during the 2016 and 2018 flood events at Locations 7 and 9 to understand the sediment transport rates at both upstream and downstream locations. Location 7 is the most downstream streamflow gauge, where hourly streamflow data can be obtained, while Location 9 is situated in the upstream reach. Both locations are adjacent to hourly streamflow gauges. As shown in Figure 4, the bedload transport rate at Location 9 (upstream) is 18 and 3 times higher than that at Location 7 (downstream) for Case 0 and 1, respectively. This difference is attributed to the steeper bed slope at Location 9 than at Location 7, as illustrated in Figure 1. The suspended transport rates obtained in Case 0 are 15–25 times higher than those obtained in Case 1 for all cases. This difference arises because Case 0 assumes a constant sediment size distribution, whereas Case 1 considers factors such as sediment inflow from upstream and bed material coarsening. This suggests that incorporating such non-equilibrium transport processes is important for rivers such as the Kelani River, where suspended sediment transport is dominant.

4.2. Sediment Grain Size Distribution

Figure 5 compares the calculated sediment size distribution for Case 1 (i.e., the RSR model results) with the observed sediment size distribution at Location 8. Location 8 was selected to analyse the sediment grain size distribution due to its location between Locations 7 and 9, which were utilized for the estimation of sediment load rates for both downstream and upstream areas, and the field-measured sediment grain size distribution data availability. Additionally, sediment distribution at Location 8 can be influenced by the sediment supply from hillslopes at the u1, u2, and u3 unit channels in the later part of this study. The computed results are presented for the bed surface, bedload, and suspended load at Location 8, at both peak discharge and the initial condition. It is interesting to note that while the sediment size distribution of the bed surface at peak discharge shows an approximately 34–43% reduction in mean diameter relative to the initial condition, the sediment size distributions of bedload and suspended load closely resemble the observed values at Location 8 with a difference in mean diameter of less than 40% for the 2016 flood event and 15% for the 2016 the 2018 flood event, respectively. Here, the mean diameter is defined with reference to Folk and Wark (1957) [34].

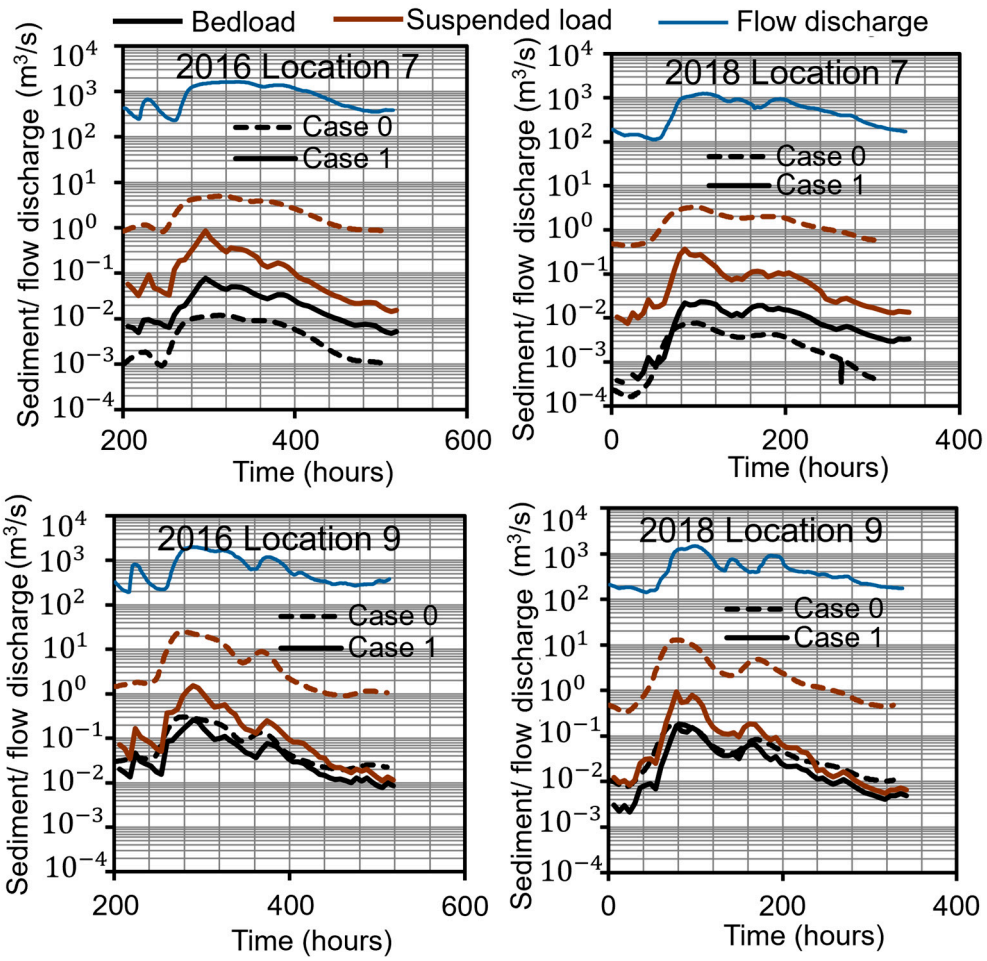


Figure 4. Comparison of Cases 0 and 1 for the bedload transport rate at Location 7 (downstream) and Location 9 (upstream).

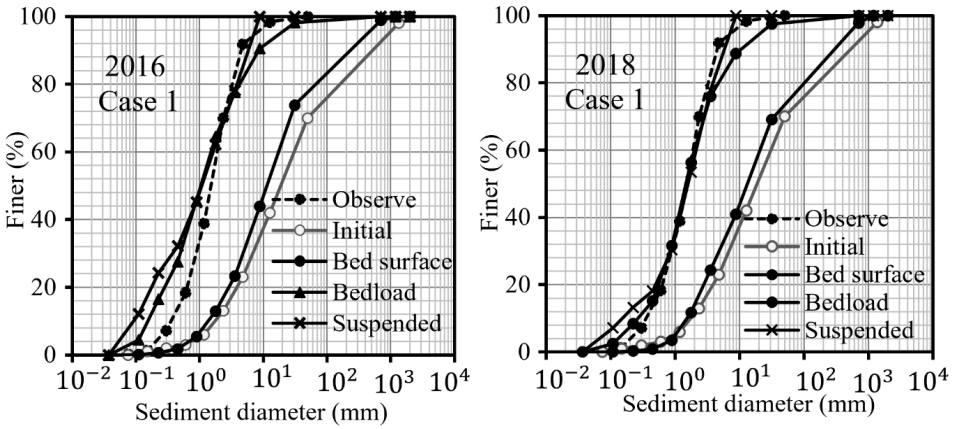


Figure 5. Sediment grain size distribution of bed surface material, bedload material, and suspended material for Case 1 with field measurement and initial condition of the calculation at Location 8.

5. Influences of Sediment Supply from Upstream Hillslopes

Figure 3 shows that in Case 1, the RSR model with no sediment supply from the end of the most upstream unit channels demonstrates good agreement with the observed data in terms of suspended sediment concentration at the Ambatale water treatment plant. It is important to note that these data were collected near an intake weir and are significantly influenced by conditions such as water extractions at the weir. Furthermore,

as shown in Figure 3, the observed sediment concentrations are very low. In addition, Figure 4 shows a substantial difference in the suspended transport rates between Case 0 (assuming equilibrium) and Case 1. These results suggest that incorporating sediment supply from hillslopes into the channel network is crucial for understanding sediment dynamics in the basin. Therefore, this section shows an analysis incorporating the sediment supply from hillslopes into the channel network. Although there are several methods for evaluating such sediment supply, this study presents a simple approach: imposing a constant sediment size distribution in several upstream unit channels. This additional calculation specifically aims to discuss the supply conditions that could reproduce the current observed bed surface sediment size distribution.

As shown in Figure 6, Location 8 in Figure 1 is selected as the target location to discuss the observed and calculated sediment size distribution. A calculation for Case 2 is conducted with sediment supply from unit channels u1, u2, and u3.

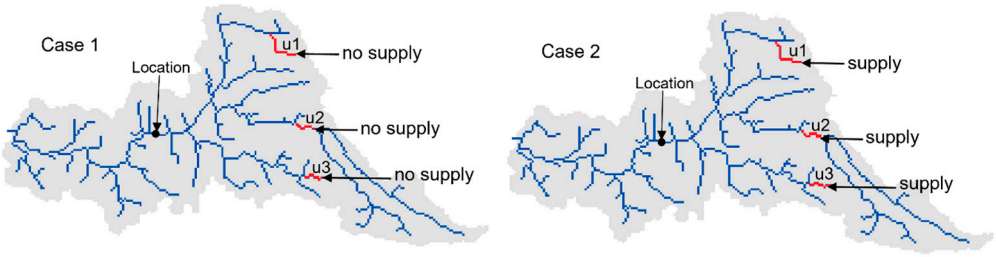


Figure 6. Outlines of Case 1 and Case 2.

For Case 1, the inflow sediment condition of unit channels u1, u2, and u3, and the temporal variations of the sediment store volume of the unit channel $\partial S_j/\partial t$ are

$$Q_{ts,x_i},\ Q_{ts,y_i} = 0,\ \partial S_j/\partial t \neq 0 \tag{12}$$

where x_i, and y_i are referred to in Figure 2. This means that the sediment supply at the uppermost unit channels is not considered, and bed erosion occurs as sediment transport occurs.

For Case 2, the inflow sediment condition of unit channels u1, u2, and u3, and the temporal variations of the sediment stored volume of unit channel $\partial S_j/\partial t$ are assumed as follows:

$$Q_{ts,x_i},\ Q_{ts,y_i} \neq 0,\ \partial S_j/\partial t = 0 \tag{13}$$

This means that in Case 2, the sediment size distributions at unit channels u1, u2, and u3 are constant in time, and bed deformation is not considered in these unit channels. This is a simple sediment supply condition from these unit channels.

The sediment grain size distribution of the bed surface material at Location 8 in Cases 1 and 2 is evaluated to elucidate the bed surface material composition in relation to the sediment supply from the end of the upstream unit channels. Figure 7 compares the sediment grain size distribution and mean diameter of the bed surface, bedload, and suspended load material for Cases 1 and 2 during the 2016 and 2018 flood events. Figure 7A compares the sediment grain size distribution of the bed surface, bedload, and suspended load material for Cases 1 and 2 at the peak discharge, along with the initial sediment grain size distribution of the RSR model and the field-measured sediment grain size distribution at Location 8. As shown in Figure 7A, the sediment grain size distribution of the bed surface material in Case 2 exhibits a composition of finer sediment (<2 mm) that is 4–5 times higher than that of the bed surface material in Case 1 and the initial sediment grain size distribution of the RSR model. Furthermore, the Case 2 results more closely approximate the field-measured sediment size distribution at this location, with a mean

diameter difference of 0.29 mm. Both distributions are very well sorted and Leptokurtic, with a standard deviation difference of 0.2, and a Kurtosis difference of 0.2, as referenced by Folk and Ward (1957) [34]. These results suggest that the bed surface stratum is enhanced due to the fine sediment supply originating from the most upstream unit channel. The bedload and suspended materials in Case 2 exhibit an increase in finer grain sizes (<2 mm) of 30% compared to those in Case 1. This difference is due to the presence of a greater proportion of fine material in the bed surface form in Case 2, resulting in a finer sediment grain-size distribution for both bedload and suspended material. Figure 7B illustrates the temporal variations in the mean diameter of the bed surface, bedload, and suspended materials for Cases 1 and 2 at Locations 8 throughout the flood period. As shown in Figure 7B, the mean diameter of the bed surface material in Case 2 decreases significantly during the flood, whereas the mean diameter of the bed surface material in Case 1 remains coarser with less variation during the flood. The mean diameter of bedload material and suspended load material in Case 1 increases during the flood, reaching more than 1 mm from an initial mean diameter of 0.1 mm, while the mean diameter of bedload material and suspended material in Case 2 remains approximately 0.1 mm even during the flood.

Temporal changes in sediment grain size distribution affect sediment transport rates. Figure 8 compares the bedload and suspended load rate variations for Cases 0, 1, and 2 during the 2016 and 2018 flood events at Locations 7 (downstream) and 9 (upstream). As shown in the Figure, bedload transport rates are 9–20 times higher in Case 2 than in Case 1. Suspended load transport rates exhibit trends similar to those of bedload transport rates, with Case 2 resulting in transport rates approximately one order of magnitude higher than those of Case 1.

Figure 9 compares the erosion and deposition in the river channel networks during the 2016 and 2018 flood events for Cases 1 and 2. In both cases, the downstream channels show deposition trends, whereas the upstream channels show erosion trends. The main channel exhibits a significant sediment deposition trend in its downstream reach, particularly downstream of Location 7. This is attributed to the notably milder bed slope in this reach, as shown in Figure 1. Table 2 presents the sediment stored volumes of channels C1 to C6, as shown in Figure 9. It is evident that sediment stored volumes are significantly higher in Case 2 than in Case 1, except for channel C1. This difference is attributed to the steep terrain in the most upstream unit channel of channel C1, where the equilibrium sediment transport is demonstrated while the adjacent unit channel is subjected to severe erosion in Figure 9. The amount of sediment deposition in the downstream reach (channel C6) in Case 2 increases by seven times compared to that in Case 1 for both the 2016 and 2018 flood due to sediment supply from hillslopes.

Table 2. Sediment stored volume (m^3) of channels C1 to C6.

Flood in 2018		Flood in 2016		Channel
Case 2	**Case 1**	**Case 2**	**Case 1**	
−1,110,000	40,000	−1,000,000	1,110,000	C1
620,000	50,000	3,530,000	−110,000	C2
350,000	30,000	670,000	70,000	C3
90,000	20,000	150,000	10,000	C4
320,000	27,000	630,000	10,000	C5
1,020,000	150,000	2,040,000	290,000	C6

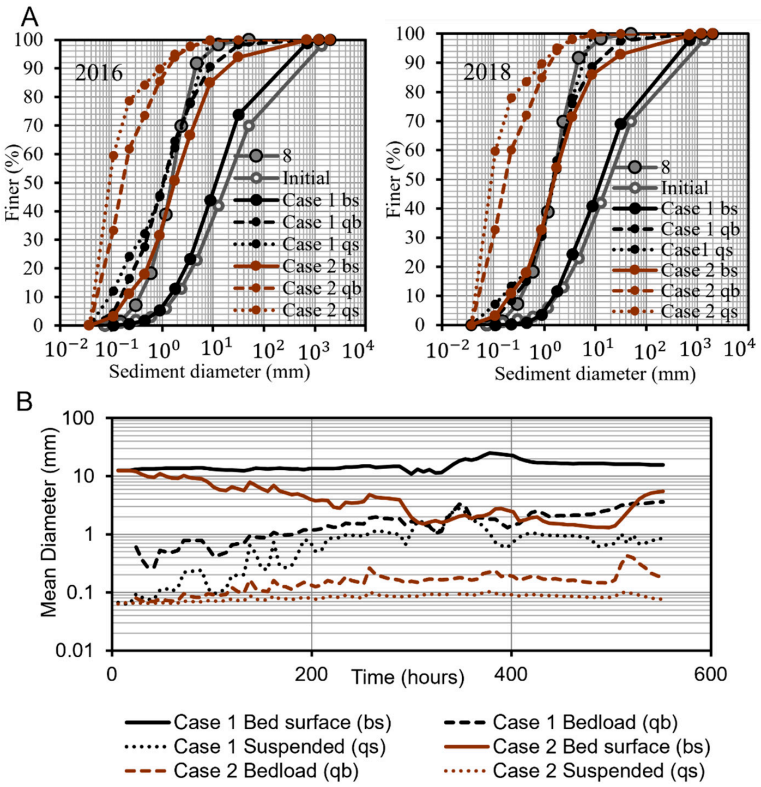


Figure 7. (**A**) Sediment grain size distribution; (**B**) Mean diameter of bed surface, bedload, and suspended load material for Cases 1 and 2 at Location 8.

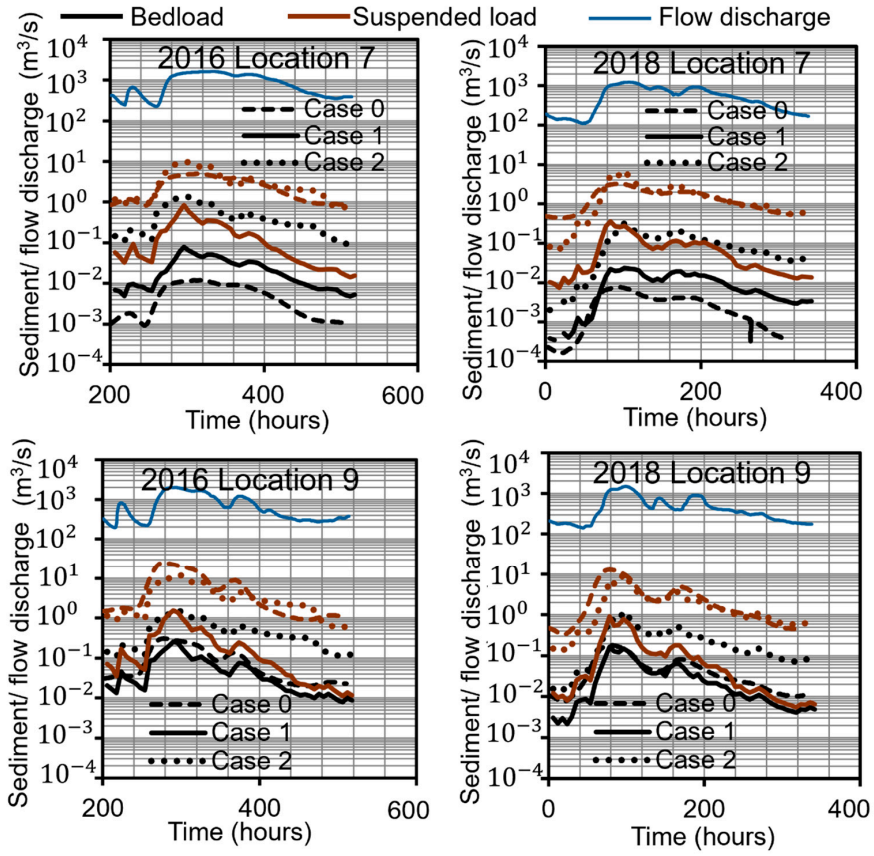


Figure 8. Bedload and suspended load rate at Location 7 (downstream) and Location 9 (upstream) for Cases 1 and 2.

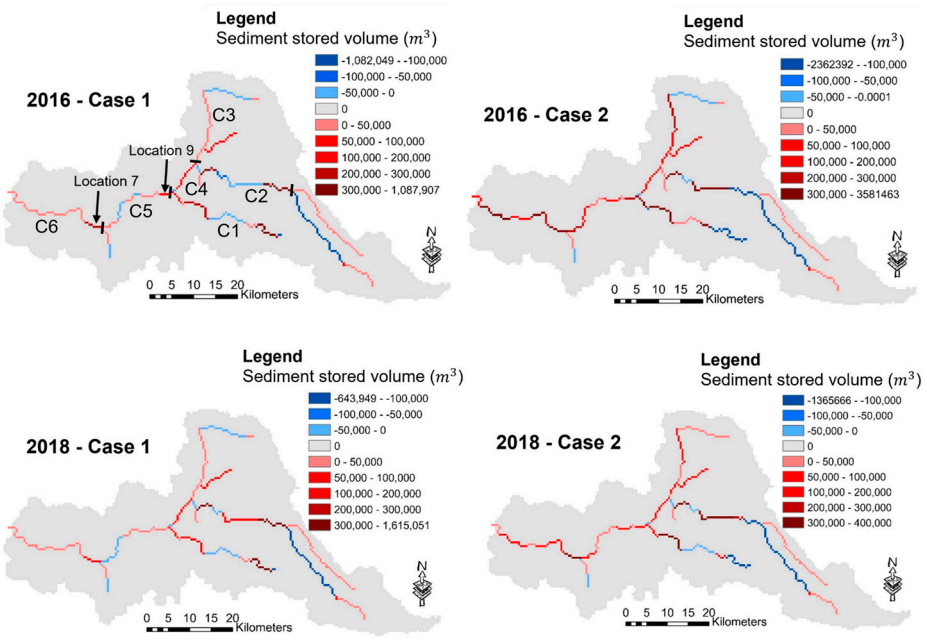


Figure 9. Deposition and erosion amount over catchment for Cases 1 and 2.

6. Discussion

This section discusses the sediment transport processes in the Kelani River, specifically the formation process of the bed material grain size distribution, by comparing three calculation cases.

Case 0: with no bed variations and constant sediment grain size distribution.

Case 1: with no sediment supply from slopes.

Case 2: with sediment supply from slopes.

The conditions for these cases are as follows: In Case 0, sediment transport estimates are conducted with no bed variations, uniform channel geometry width, and the sediment conditions are set to the field-measured sediment grain size distribution for both the downstream and upstream reaches. A constant sediment grain size distribution is maintained in the downstream and upstream reaches, with no sediment supply from the slopes. In Case 1, sediment transport estimates utilise the RSR model, with the channel geometry determined by the input Digital Elevation Model. Sediment conditions are set to the calibrated sediment grain size distribution as the initial sediment grain size of the channel bed in the river network. The sediment grain size distribution changes temporally and spatially depending on variations in sediment transport rates, channel characteristics, and flow, assuming no sediment supply from the slopes. The only difference between Cases 1 and 2 is that Case 2 incorporates sediment supply from hillslopes at the ends of the most upstream unit channels.

As shown in Figure 8, the bedload and suspended transport rates in Case 1 are approximately one order of magnitude smaller than those in Case 2. This indicates that without sediment supply from the hillslopes, the bed sediment size distribution rapidly coarsens, even with a single flood event. The condition in Case 2, where the grain size distribution in unit channels u1, u2, and u3 remains constant over time, means that the bed material transported by the flow is immediately replenished by the sediment supplied from the hillslopes. In other words, such an amount of sediment supply, i.e., a sufficient amount to maintain a constant sediment size distribution in unit channels u1, u2, and u3, contributes to the formation of the current bed sediment size distribution in the downstream reaches.

Regarding this formation process, it is interesting to note that in Case 2, as shown in Figure 7, the sediment size distributions are close to the observed values, with a mean diameter difference of less than 0.29 mm. Both distributions are very well sorted and Leptokurtic, with a standard deviation difference of less than 0.2, and a Kurtosis difference of less than 0.2, as referenced by Folk and Ward (1957) [34] for both 2016 and 2018 flood events, regardless of the flood magnitude. This suggests that with a sufficient amount of sediment supply, the bed material sediment size distribution is formed based on channel conditions such as the width and slope at that location. This could be further discussed through sensitivity analysis by varying the initial bed material size distribution and flow magnitudes.

Considering that the observed bed material sediment size distribution does not change rapidly over time, a simplified evaluation of the sediment transport capacity using manual calculations, as in Case 0, which assumes a constant sediment size distribution of the observed bed material, provides valuable information for river channel management. On the other hand, calculations for the spatiotemporal distribution of bedload transport, suspended load transport, and bed deformation, as in the RSR model, also provide insights for effective and sustainable river management and sand mining activities. Notably, as shown in Figures 1 and 9, the Kelani River exhibits a tendency for sediment deposition downstream at Location 7. Therefore, analyses such as Case 2 are beneficial for understanding measures to restore riverbed elevation and gain insights for sustainable river management and sand mining.

7. Conclusions

This study investigates the characteristics of sediment transport in the Kelani River Basin during floods using three different calculation methods, with a particular focus on the formation process of the bed material grain size distribution in the downstream reach. The conclusions are as follows:

1. The RSR model results indicate a significant sediment deposition trend in the downstream reach, particularly the downstream reach of Location 7. Case 2 results exhibit bedload and suspended transport rates in the downstream reach approximately one order of magnitude higher than those in Case 1, which does not consider hillslope sediment supply. In Case 1, the sediment size distribution in the downstream reach rapidly coarsens.
2. In Case 2, which incorporates the sediment supply, the bed sediment size distribution in the downstream reach is close to the observed size distribution, regardless of the flood magnitude. This suggests that with a sufficient amount of sediment supply, the bed material sediment size distribution is formed based on channel conditions such as the width and slope at that location.
3. While simplified evaluation of sediment transport capacity using manual calculations, as in Case 0 (assuming a constant grain size distribution), provides valuable information for river management, the RSR model offers advantages by calculating the spatiotemporal distribution of bedload transport, suspended load transport, and bed deformation. This provides insights for effective and sustainable river management and sand mining activities. Therefore, analyses such as Case 2 are also beneficial for understanding measures to restore riverbed elevation and gain insights for sustainable river management and sand mining.

Author Contributions: Conceptualization, P.S.D.M. and D.H.; Data curation, P.S.D.M.; Formal analysis, P.S.D.M.; Funding acquisition, Y.I.; Investigation, P.S.D.M.; Methodology, P.S.D.M., D.H. and S.E.; Project administration, P.S.D.M. and Y.I.; Resources, P.S.D.M.; Software, P.S.D.M. and D.H.;

Supervision, Y.I. and S.E.; Validation, P.S.D.M. and D.H.; Visualization, P.S.D.M.; Writing—original draft, P.S.D.M.; Writing—review and editing, D.H. All authors have read and agreed to the published version of the manuscript.

Funding: This research was funded by the Tokyo Metropolitan Government, grant number (R4-2).

Data Availability Statement: The original contributions presented in this study are included in the article. Further inquiries can be directed to the corresponding authors.

Acknowledgments: The authors express gratitude to the Irrigation Department, Meteorological Department, National Water Supply and Drainage Board, Sri Lanka, for providing data; the Department of Civil Engineering of the University of Moratuwa for access to laboratory facilities used in wet and dry sieve analysis; Toru Konishi for his comments; and Hideo Amaguchi for assistance with the software.

Conflicts of Interest: The authors declare no conflicts of interest.

References

1. Pathmalal, M.; Yohan, L.M.; Roshan, A.; Sampath, A.; Visitha, I.A. The Need for Proper Management Leading to the Sustainability of the Kelani River and Its Lower Basin. *J. Water Land Dev.* **2020**, *47*, 10–15.
2. Narangoda, C.; Amarathunga, D.; Deepani Dangalle, C. Evaluation of Water Quality in the Upper and Lower Catchments of the Kelani River Basin, Sri Lanka. *Water Pract. Technol.* **2023**, *18*, 716. [CrossRef]
3. Narangoda, C.N.K.; Dangalle, C.D.; Amarathunga, D. Selected Freshwater Fish Species for Assessing the Water Quality of the Lower Catchment of the Kelani River, Sri Lanka. *Environ. Monit. Assess.* **2022**, *194*, 650. [CrossRef] [PubMed]
4. Surasinghe, T.; Kariyawasam, R.; Sudasinghe, H.; Karunarathna, S. Challenges in Biodiversity Conservation in a Highly Modified Tropical River Basin in Sri Lanka. *Water* **2019**, *12*, 26. [CrossRef]
5. Abeysinghe, N.M.D.A.; Samarakoon, M.B. Analysis of Variation of Water Quality in Kelani River, Sri Lanka. *Int. J. Environ. Agric. Biotechnol.* **2017**, *2*, 2770–2775. [CrossRef]
6. Wickramasinghe, W.C.N. River Profile Kelani River-Sri Lanka. 2018. Available online: https://www.scribd.com/document/447580431/River-Profile-Kelani-River-Sri-Lanka (accessed on 25 November 2024).
7. Friend, P.F. Control of River Morphology by the Grain-Size of Sediment Supplied. *Sediment. Geol.* **1993**, *85*, 171–177. [CrossRef]
8. Zhang, L.; Zhang, H.; Tang, H.; Zhao, C. Particle Size Distribution of Bed Materials in the Sandy River Bed of Alluvial Rivers. *Int. J. Sediment Res.* **2017**, *32*, 331–339. [CrossRef]
9. Einstein, H.A. *The Bed-Load Function for Sediment Transportation in Open Channel Flows*; US Department of Agriculture: Washington, DC, USA, 1950.
10. Lanzoni, S.; Tubino, M. Grain Sorting and Bar Instability. *J. Fluid Mech.* **1999**, *393*, 149–174. [CrossRef]
11. Florsheim, J.L.; Pellerin, B.A.; Oh, N.H.; Ohara, N.; Bachand, P.A.M.; Bachand, S.M.; Bergamaschi, B.A.; Hernes, P.J.; Kavvas, M.L. From Deposition to Erosion: Spatial and Temporal Variability of Sediment Sources, Storage, and Transport in a Small Agricultural Watershed. *Geomorphology* **2011**, *132*, 272–286. [CrossRef]
12. Slattery, M.C.; Phillips, J.D. Controls on Sediment Delivery in Coastal Plain Rivers. *J. Environ. Manag.* **2011**, *92*, 284–289. [CrossRef]
13. Staudt, F.; Mullarney, J.C.; Pilditch, C.A.; Huhn, K. Effects of Grain-Size Distribution and Shape on Sediment Bed Stability, near-Bed Flow and Bed Microstructure. *Earth Surf. Process. Landf.* **2019**, *44*, 1100–1116. [CrossRef]
14. Duan, X.; Wang, Z.; Xu, M.; Zhang, K. Effect of Streambed Sediment on Benthic Ecology. *Int. J. Sediment Res.* **2009**, *24*, 325–338. [CrossRef]
15. The ASCE Task Committee on Sediment Transport and Aquatic Habitats; Sedimentation Committee. Sediment and Aquatic Habitat in River Systems. *J. Hydraul. Eng.* **1992**, *118*, 669–687. [CrossRef]
16. Pfeiffer, A.M.; Finnegan, N.J.; Willenbring, J.K. Sediment Supply Controls Equilibrium Channel Geometry in Gravel Rivers. *Proc. Natl. Acad. Sci. USA* **2017**, *114*, 3346–3351. [CrossRef]
17. Venditti, J.G.; Dietrich, W.E.; Nelson, P.A.; Wydzga, M.A.; Fadde, J.; Sklar, L. Effect of Sediment Pulse Grain Size on Sediment Transport Rates and Bed Mobility in Gravel Bed Rivers. *J. Geophys. Res. Earth Surf.* **2010**, *115*, 3039. [CrossRef]
18. Buffington, J.M.; Montgomery, D.R. Effects of Sediment Supply on Surface Textures of Gravel-Bed Rivers. *Water Resour. Res.* **1999**, *35*, 3523–3530. [CrossRef]
19. Cui, Y.; Parker, G.; Lisle, T.E.; Gott, J.; Hansler-Ball, M.E.; Pizzuto, J.E.; Allmendinger, N.E.; Reed, J.M. Sediment Pulses in Mountain Rivers: 1. Experiments. *Water Resour. Res.* **2003**, *39*. [CrossRef]
20. Cui, Y.; Parker, G.; Pizzuto, J.; Lisle, T.E. Sediment Pulses in Mountain Rivers: 2. Comparison between Experiments and Numerical Predictions. *Water Resour. Res.* **2003**, *39*, 1240. [CrossRef]

21. Egashira, S.; Matsuki, K. A Method for Predicting Sediment Runoff Caused by Erosion of Stream Channel Bed. *Proc. Hydraul. Eng.* **2000**, *44*, 735–740. [CrossRef]
22. Harada, D.; Egashira, S. Methods to Evaluate Sediment and Driftwood Laden Flood -In the Akatani River Flood Disaster in July 2017-. In Proceedings of the 39th IAHR World Congress, Granada, Spain, 19–24 July 2022.
23. Rahman, M.M.; Harada, D.; Egashira, S. Sediment Transport Processes in the Sangu River Basin Using a Rainfall-Sediment Runoff Model for Sustainable River Management. *Proc. IAHS* **2024**, *386*, 109–114. [CrossRef]
24. Dissanayaka, K.D.C.R.; Rajapakse, R.L.H.L. Long-Term Precipitation Trends and Climate Extremes in the Kelani River Basin, Sri Lanka, and Their Impact on Streamflow Variability under Climate Change. *Paddy Water Environ.* **2019**, *17*, 281–289. [CrossRef]
25. SCRIP. *Climate Resilience Improvement Project; Strategic Environmental Assessment of Development of River Basin Level Flood and Drought Mitigation Investment Plans (DBIP)*; Consulting Engineers & Architects Associated (Pvt.) Ltd.: Kotte, Sri Lanka, 2018.
26. Hettiarachchi, P. Flood Frequency Analysis for the Kelani River and the Design Flood for Kelani Flood Bunds. Available online: https://www.researchgate.net/publication/327745195_Flood_Frequency_Analysis_for_the_Kelani_River_and_the_Design_Flood_for_Kelani_Flood_Bunds (accessed on 21 May 2023).
27. De Silva, M.M.G.T.; Weerakoon, S.B.; Herath, S.; Ratnayake, U.R.; Mahanama, S. Flood Inundation Mapping along the Lower Reach of Kelani River Basin under the Impact of Climate Change. *Eng. J. Inst. Eng. Sri Lanka* **2012**, *45*, 23. [CrossRef]
28. Meyer-Peter, E.; Muller, R. Formulas for Bed-Load Transport. In Proceedings of the Second Meeting International Association for Hydraulic Structures Research, Stockholm, Sweden, 7–9 June 1948; pp. 39–64.
29. Brown, C.B. Sediment Transportation. In *Engineering Hydraulics*; Hunter, R., Ed.; Wiley: New York, NY, USA, 1950; pp. 769–857.
30. Egashira, S.; Miyamoto, K.; Ito, T. Bed-Load Rate in View of Two Phase Flow Dynamics. *Proc. Hydraul. Eng.* **1997**, *41*, 789–794. [CrossRef]
31. Egashira, S.; Itoh, T. Paradoxical Discussions on Sediment Transport Formulas. In *River, Coastal and Estuarine Morphodynamics RCEM 2005, Proceedings of the 4th IAHR Symposium on River, Coastal and Estuarine Morphodynamics, Urbana, IL, USA, 4–7 October 2005*; Springer: Berlin/Heidelberg, Germany, 2005; Volume 1, pp. 33–38.
32. Harada, D.; Egashira, S.; Ahmed, T.S.; Ito, H. Entrainment of Bed Sediment Composed of Very Fine Material. *Earth Surf. Process. Landf.* **2022**, *47*, 3051–3061. [CrossRef]
33. Egashira, S.; Ashida, K. Studies on the Structures of Density Stratified Flows. *Bull. Disaster Prev. Res. Inst.* **1980**, *29*, 165–198.
34. Blott, S.J.; Pye, K. Gradistat: A Grain Size Distribution and Statistics Package for the Analysis of Unconsolidated Sediments. *Earth Surf. Process. Landf.* **2001**, *26*, 1237–1248. [CrossRef]

Disclaimer/Publisher's Note: The statements, opinions and data contained in all publications are solely those of the individual author(s) and contributor(s) and not of MDPI and/or the editor(s). MDPI and/or the editor(s) disclaim responsibility for any injury to people or property resulting from any ideas, methods, instructions or products referred to in the content.